Molecular Biology of the Cell
Vol. 16, 1120–1130, March 2005

The Rate-limiting Enzyme in Phosphatidylcholine Synthesis Regulates Proliferation of the Nucleoplasmic Reticulum[D]

Thomas A. Lagace* and Neale D. Ridgway

Atlantic Research Center, Departments of Pediatrics and Biochemistry and Molecular Biology, Dalhousie University, Halifax, Nova Scotia, Canada B3H 4H7

Submitted October 7, 2004; Revised December 2, 2004; Accepted December 16, 2004
Monitoring Editor: Jean Gruenberg

The nucleus contains a network of tubular invaginations of the nuclear envelope (NE), termed the nucleoplasmic reticulum (NR), implicated in transport, gene expression, and calcium homeostasis. Here, we show that proliferation of the NR, measured by the frequency of NE invaginations and tubules, is regulated by CTP:phosphocholine cytidylyltransferase-α (CCTα), the nuclear and rate-limiting enzyme in the CDP–choline pathway for phosphatidylcholine (PtdCho) synthesis. In Chinese hamster ovary (CHO)-K1 cells, fatty acids triggered activation and translocation of CCTα onto intranuclear tubules characteristic of the NR. This was accompanied by a twofold increase in NR tubules quantified by immunostaining for lamin A/C or the NE. CHO MT58 cells expressing a temperature-sensitive CCTα allele displayed reduced PtdCho synthesis and CCTα expression and minimal proliferation of the NR in response to oleate compared with CHO MT58 cells stably expressing CCTα. Expression of CCTα mutants in CHO58 cells revealed that both enzyme activity and membrane binding promoted NR proliferation. In support of a direct role for membrane binding in NR tubule formation, recombinant CCTα caused the deformation of liposomes into tubules in vitro. This demonstrates that a key nuclear enzyme in PtdCho synthesis coordinates lipid synthesis and membrane deformation to promote formation of a dynamic nuclear-cytoplasmic interface.

INTRODUCTION

Biological membranes undergo fusion and formation of polymorphic structures that are dependent on lipid composition and associated proteins. As an example, membrane trafficking involves fusion events and formation of vesicular and tubular structures that is controlled by phospholipid composition (de Figueiredo *et al*., 2001; Drecktrah *et al*., 2003), reversibly polymerizing protein coats (Rothman and Wieland, 1996; Bigay *et al*., 2003) and amphipathic proteins that insert into bilayers (Ford *et al*., 2002; Peter *et al*., 2004). Although it has been established that catalytic amounts of regulatory lipids such as diacyglycerol (DAG), poly-phosphatidylinositols, and phosphatidic acid can regulate membrane dynamics (Fang *et al*., 1998), the role that more abundant lipids or their biosynthetic enzymes play in this process is unknown. A potentially important enzyme in this process is CTP:phosphocholine cytidylyltransferase (CCT), which catalyzes the rate-limiting reaction in the CDP–choline pathway for biosynthesis of phosphatidylcholine (PtdCho), the most abundant phospholipid in membranes (Kent, 1997) (Figure 1). The capacity of CCT to reversibly bind membranes (Cornell and Northwood, 2000) and regulate synthesis of PtdCho at these sites suggests a key role in altering membrane structure and function.

Two human CCT genes encode CCTα and the CCTβ1 and β2 isoforms, respectively (Lykidis and Jackowski, 2001). Unlike the CCTβ isoforms, which display restricted tissue distribution and are primarily expressed in the cytoplasm, CCTα is ubiquitously expressed and is localized in the nucleus by virtue of a N-terminal nuclear localization signal (Wang *et al*., 1995; DeLong *et al*., 2000) (Figure 1). CCTα is an amphitrophic enzyme, existing as both soluble inactive and membrane-bound active forms (Cornell and Northwood, 2000). Thus, in Chinese hamster ovary (CHO), HeLa, and liver cells, nucleoplasmic CCTα translocates to the nuclear envelope (NE) in response to numerous stimuli, including fatty acids (Wang *et al*., 1993), PtdCho degradation by phospholipase C (Watkins and Kent, 1992), and isoprenoids (Lagace *et al*., 2002). Adjacent to the CCTα catalytic domain is a 50-amino acid amphipathic helix (domain M) with interfacial lysine residues that inserts into membranes in response to activating lipids such as fatty acids or DAG (Cornell, 1998; Johnson *et al*., 2003a) (Figure 1). These activating lipids increase membrane lateral packing stress or negative charge, resulting in domain M insertion into the bilayer (Attard *et al*., 2000). The product of the CDP–choline pathway, PtdCho, reduces bilayer lateral packing stress, whereas lipid precursors of the pathway promote increased head-

This article was published online ahead of print in *MBC in Press* (http://www.molbiolcell.org/cgi/doi/10.1091/mbc.E04–10–0874) on January 5, 2005.

[D] The online version of this article contains supplemental material at *MBC Online* (http://www.molbiolcell.org).

* Present address: Department of Molecular Genetics, University of Texas Southwestern Medical Center, Dallas, TX 75390.

Address correspondence to: Neale D. Ridgway (nridgway@dal.ca).

Abbreviations used: CK, choline kinase, Con A, concanavalin A; CPT, choline phosphotransferase; CCT, CTP:phosphocholine cytidylyltransferase; DAG, diacylglycerol; EM, electron microscopy; LPDS; lipoprotein deficient serum; NE, nuclear envelope; NR, nucleoplasmic reticulum; NPC, nuclear pore complex; PtdCho, phosphatidylcholine; PDI, protein disulfide isomerase.

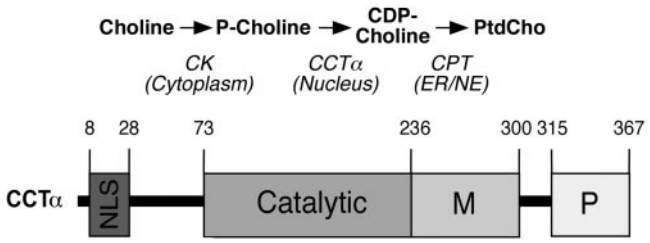

Figure 1. CDP–choline pathway and domain organization of CCTα. M, domain M; P, phosphorylation domain; NLS, nuclear localization signal.

group spacing or negative character and thus favor CCTα insertion into membranes. This provides a homeostatic mechanism whereby CCTα "senses" the status of membranes with respect to content of PtdCho and CDP–choline pathway substrates such as DAG and fatty acids.

The biological relevance of nuclear localization of CCTα is unknown, but it could be important for coordinating PtdCho synthesis with the cell cycle (Jackowski, 1996), sequestering inactive CCTα (Northwood *et al*., 1999), or regulating an endonuclear pool of PtdCho involved in chromatin function (Hunt *et al*., 2001). Choline phosphotransferase (CPT), which catalyzes the terminal step in the CDP–choline pathway (Figure 1), has been found on the NE as well as the ER (Henneberry *et al*., 2002). This suggests that the NE could be a major site of PtdCho synthesis after activation and membrane translocation of nuclear CCTα. However, the possibility that CCTα translocation could affect NE morphology, either via direct membrane binding or by increasing localized PtdCho synthesis, has not been investigated. A notable feature of the NE are double membrane invaginations, termed the nucleoplasmic reticulum (NR), which have a lumen contiguous with the cytoplasm (Fricker *et al*., 1997; Broers *et al*., 1999; Echevarria *et al*., 2003). These invaginations frequently traverse the entire nucleus in a vertical orientation, are branched, and contain nuclear pore complexes (NPCs). The precise function of the NR is unknown, although it has been shown to be a site of localized Ca^{2+} release and protein kinase C activation (Lui *et al*., 1998; Echevarria *et al*., 2003). NE invaginations also have been proposed to facilitate transport processes by extending the nuclear-cytoplasmic interface to specific intranuclear sites, such as nucleoli (Fricker *et al*., 1997), or by increasing the surface/volume ratio of the nucleus (Johnson *et al*., 2003b). NR tubules are generally surrounded by the nuclear lamina that also underlies the peripheral NE and thus could provide structural support within the nucleus or affect chromatin organization dependent on lamin-DNA contacts (Broers *et al*., 1999).

The NR is variably expressed in normal and transformed cells and undergoes dynamic changes in morphology and distribution over a time scale of minutes (Fricker *et al*., 1997). Although the morphology of the NR is well characterized, factors that control expression and proliferation of this membrane network are poorly understood. Here, we show that CCTα associates with the NR and that nuclear tubules characteristic of the NR increased in response to both CCTα activation and expression, and direct membrane deforming properties of the enzyme. These results indicate a novel role for CCTα and the CDP–choline pathway in regulating a dynamic membrane network involved in diverse aspects of nuclear function.

MATERIALS AND METHODS

Materials

Bovine serum albumin (BSA) (fraction V, essentially fatty acid free) and goat anti-rabbit IgG conjugated to 10-nm colloidal gold were purchased from Sigma-Aldrich (St. Louis, MO). Phosphatidylethanolamine (PtdEtn, egg), PtdCho (egg), phosphatidylserine (PtdSer, brain), phosphatidylinositol 4-phosphate (PtdIns-4-P, brain), and total brain phospholipids (bovine) were obtained from Avanti Polar Lipids (Alabaster, AL). [methyl-^{3}H]Choline and phospho[*methyl*-^{14}C]choline were from Mandel-New England Nuclear (Boston, MA). Cell culture medium and reagents were from Invitrogen (Carlsbad, CA). Recombinant rat CCTα expressed in the baculovirus system was provided by Rosemary Cornell (Simon Fraser University, Vancouver, British Columbia, Canada). Lipoprotein-deficient serum (LPDS) was prepared from fetal calf serum (FCS) by centrifugation at 150,000 × *g* for 26 h, followed by extensive dialysis against 10 mM phosphate, pH 7.4, and 150 mM NaCl (Goldstein *et al*., 1983). Stock solutions of arachidonic acid and oleic acid (10 mM) (Matreya, State College, PA) were prepared by dilution in ethanol and conversion to the sodium salt by addition of NaOH. The sodium salt was then evaporated under N_2, dissolved in 150 mM NaCl and BSA [10% (wt/vol)], and stirred at room temperature for 10 min. A monoclonal antibody (mAb) (131C3) against a common epitope in lamin A and C was supplied by Dr. Yves Raymond (Université de Montreal, Montreal, Montreal, Canada). A mAb to protein disulfide isomerase (PDI) was from StressGen Biotechnologies (San Diego, CA). mAb 414 directed against a common epitope in Nup62 and related components of the NPC was from Babco (Richmond, CA). Alexafluor-conjugated secondary antibodies, Alexaflour-conjugated concanavalin A (Con A), and Oregon green 488-conjugated dextran (70 kDa) were from Molecular Probes (Eugene, OR)

Cell Culture

CHO-K1 cells (ATCC CCL61) were cultured in DMEM with 5% FCS and proline (34 μg/ml) in an atmosphere of 5% CO_2 at 37°C. CHO MT58 cells were cultured in medium A at 33°C. NIH 3T3 and F8 fibroblasts were cultured in DMEM with 10% FCS. All cells were cultured in DMEM with 5% LPDS for 24 h before the start of experiments.

CHO MT58 cells overexpressing CCTα (CHO58-CCT) and vector-transfected controls cells (CHO58-Vec) were described previously (Houweling *et al*., 1995). CHO MT58 cells overexpressing V5 epitope-tagged CCTα and CCTα mutants were prepared by calcium phosphate transfection with pcDNA3.1/V5His-CCT, pcDNA3.1/V5His-CCT H89G, pcDNA3.1/V5His-CCT K122A, or pcDNA3.1/V5His-CCTΔ236. Stably transfected cells were selected in DMEM with 10% FCS, proline (34 μg/ml), and G418 (800 μg/ml). Pools of individual colonies (>100) were screened for expression by immunofluorescence detection with an anti-V5 mAb. Optimally expressing pools of cells (>90%) were maintained in medium containing G418 (400 μg/ml). Control cells were prepared by transfection with empty vector and selected as described above.

CCTα and PtdCho Synthesis

CCTα activity in soluble and membrane fractions was assayed in the presence of PtdCho-oleate vesicles by monitoring the conversion of phospho[^{3}H]choline to CDP-[^{3}H]choline (Cornell and Vance, 1987). The synthesis of PtdCho in cultured cells was determined by pulse-labeling with [^{3}H]choline as described previously (Storey *et al*., 1998).

CCTα was detected by immunoblotting of cell extracts using polyclonal antibody directed against the C-terminal phosphorylation domain or N-terminus (Yang *et al*., 1997). Blots were incubated with goat anti-rabbit horseradish peroxidase-conjugated secondary antibody and visualized by the chemiluminescence method (Amersham Biosciences, Piscataway, NJ).

Immunofluorescence microscopy

Cells were cultured on glass coverslips to 50% confluence, fixed in 3% formaldehyde, and permeabilized with 0.05% (wt/vol) Triton X-100 for 10 min at −20°C. In experiments investigating localization of lamin A/C, cells were fixed and permeabilized on glass coverslips in cold methanol/acetone [1:1 (vol/vol)] for 15 min at −20°C. For all experiments, coverslips were blocked with 1% (wt/vol) BSA in phosphate-buffered saline (PBS) (10 mM Na_2HPO_4, pH 7.4, 225 mM NaCl, and 2 mM $MgCl_2$) for 30 min before incubation with primary and secondary Alexafluor-conjugated antibodies (see figure legends for details). After final washes, coverslips were mounted in 50 mM Tris-HCl, pH 9.0, 2.5% (wt/vol) 1,4-diazabicyclo-[2.2.2]-octane, and 90% (vol/vol) glycerol and viewed using a Zeiss confocal microscope model LSM510 or LSM 510 Meta equipped with a 100× oil immersion objective. LSM510 Meta and Adobe Photoshop software were used for image projections and reconstruction of XZ and YZ planes from 18 to 20 serial Z-axis scans of 0.5–0.6 μm. When labeling with Alexa488-conjugated Con A, coverslips were incubated for 15 min in Con A (2 μg/ml) in 1% (wt/vol) BSA in PBS. Oregon green 488-labeled dextran was introduced into CHO-K1 cells by scrape loading (Fricker *et al*., 1997). Coverslips were then fixed and permeabilized in 3%

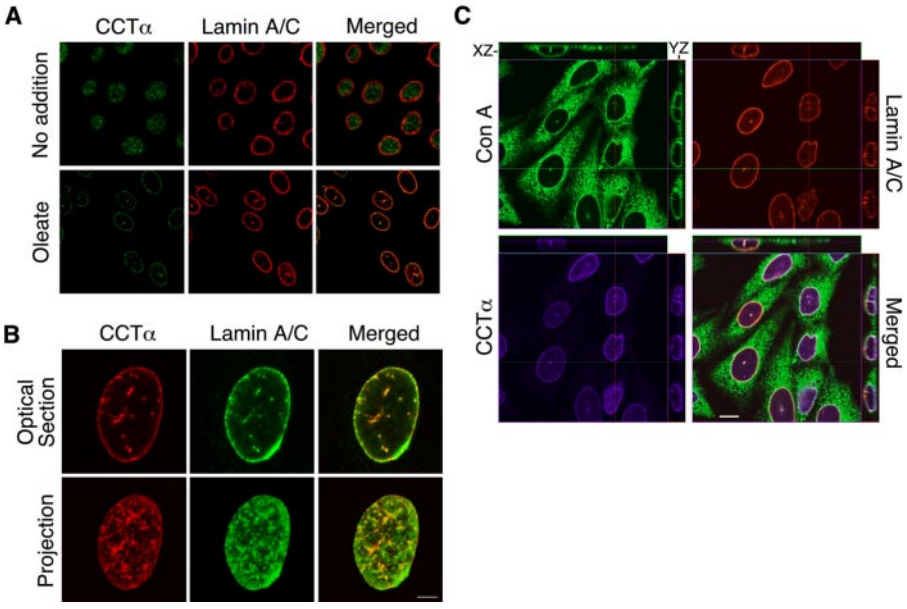

Figure 2. CCTα association with the nucleoplasmic reticulum in oleate-treated CHO-K1 cells. (A) CHO-K1 cells were treated with or without oleate (500 μM) for 4 h, fixed and permeabilized in cold MeOH/acetone, and CCTα and lamin A/C were detected using secondary antibodies conjugated to Alexa555 and Alexa488, respectively. Single optical sections are shown. (B) Projection of the nucleus of an oleate-treated CHO-K1 cells (as described in A) constructed from 20 consecutive optical sections. (C) Oleate-treated CHO-K1 cells were labeled with Alexa488-conjugated Con A, and CCTα and lamin A/C were visualized using Alexa647- and Alexa555-conjugated secondary antibodies, respectively. A single optical section shows the XY plane, and a series of consecutive optical sections spanning the nucleus were used to reconstruct the YZ plane (sides) and XZ plane (top). The green line shows the position of the XZ plane; the red line shows the position of the YZ plane. Bars, 10 μm.

formaldehyde and 0.05% Triton X-100 and processed for immunofluorescence as described above.

Two markers, lamin A/C and Con A, were used to identify and quantify tubules of the NR. First, lamin A/C immunostaining was examined in three-dimensional reconstructions of serial optical Z-sections (18–20 sections, 0.5–0.6 μm in thickness) spanning the nucleus (for example, see Figure 2C). Filamentous lamin A/C-positive structures continuous with the peripheral NE and spanning >50% of the nuclear volume were scored (method used for quantification in Figure 4A). Second, based on three-dimensional reconstructions of serial Z-sections of nuclei stained with Alexa488-conjugated Con A (Figure 2C), it was verified that intranuclear foci in single optical sections (0.5 μm) of the midnuclear region corresponded to tubular NE invaginations spanning >50% of the nucleus (for example, see Figure 2C). To facilitate screening of larger data sets (>400 cells), single optical Z-sections of the midnuclear region of cells were collected for quantification of intranuclear Con A-positive, NE-associated intranuclear tubules (Figure 4B). Compared with lamin A/C, more tubules were scored by the Con A method, but the relative increases in tubule numbers were similar (1.5- to 2-fold for both oleate-treated and control; Figure 4, A and B). It should be noted that this method scored larger extended tubules and thus provided a conservative estimate of tubule proliferation. Laser intensity was optimized for visualization of lamin and Con A and held constant for all samples within an experimental set. Data sets were collected from cells in randomly selected fields and tubules were counted by blinded and unblinded observers.

Thin Section Electron Microscopy (EM)

CHO cells were cultured to 70% confluence on 60-mm dishes and fixed in situ with 2.5% (wt/vol) glutaraldehyde in 0.1 M sodium cacodylate buffer, pH 7.2, for 1 h at room temperature. Cells were collected by scraping with a rubber policeman, sedimented by centrifugation at 1000 × *g* for 2 min, and preserved in fresh fixative overnight (Garduno *et al.*, 1998). Samples were postfixed in 2% (wt/vol) osmium tetroxide in cacodylate buffer and embedded in epoxy resin TAAB 812 (Marivac, St. Laurent, Québec, Canada). Ultrathin sections (80–100 nm) were poststained with 2% (wt/vol) uranyl acetate and lead citrate and applied to 300-mesh copper coated grids and viewed using a Philips EM300 electron microscope.

For immunoelectron microscopy, cells were fixed as described above, but in 4% paraformaldehyde, 0.5% glutaraldehyde with omission of osmium tetroxide postfixation. Ultrathin sections mounted on 200-mesh nickel grids were floated on drops of 1 mg/ml freshly prepared sodium borohydride for 10 min followed by 10-min incubation on 30 mM glycine in 0.1 M borate buffer, pH 9.6. Grids were then blocked in Tris-buffered saline (TBS) containing 1% BSA for 45 min, rinsed briefly on drops of TBS, and incubated with anti-CCTα antibody (1:1000 dilution) in TBS overnight at 4°C. Controls consisted of preimmune serum or no primary antibody. The grids were incubated for 2 h with affinity-purified goat anti-rabbit IgG conjugated to 10-nm colloidal gold. Grids were fixed for 15 min in 2.5% glutaraldehyde and stained with 2% (wt/vol) uranyl acetate and lead citrate.

Liposome Preparation and Tubulation by CCTα

Liposomes (1 mg/ml) containing total brain lipid extract or a synthetic formulation (50, 25, 17.5, 5, and 2.5 mol% of PtdCho, PtdEtn, PtdSer, oleic acid, and PtdIns-4-P, respectively) were prepared by extrusion. Briefly, lipids were dried under vacuum in 50-ml round bottom flasks, sealed under N_2, and left overnight at –20°C. Lipids were resuspended in 2 ml of liposome buffer (25 mM HEPES, pH 7.4, 100 mM KCl, and 2.5 mM $MgCl_2$) for 1 h at 25°C and extruded 20 times through a 0.4-μm polycarbonate membrane (LiposoFast; Avestin, Ottawa, Ontario, Canada). To quantify protein binding, liposomes (250 μM) were incubated with recombinant CCTα or glutathione *S*-transferase (GST)-fused to the pleckstrin homology (PH) domain of oxysterol binding protein (Wyles *et al.*, 2002) (GST-PH, 2.5 μM) for 15 min at 37°C in 50 μl of liposome buffer and placed on ice. Reactions were subjected to centrifugation at 125,000 × *g* for 20 min, supernatants were removed immediately, and pellets were resuspended in an equal volume of buffer. Proteins were resolved on SDS-10% PAGE and visualized by Coomassie staining. For EM studies, liposomes were incubated as described above, applied to Formvar and copper-coated grids (200-mesh), and negatively stained with 2% uranyl acetate.

RESULTS

Fatty Acid-activated CCTα Translocates to the Nucleoplasmic Reticulum

To test whether CCTα associates with the NR, CHO-K1 cells were cultured in lipoprotein-deficient medium for 24 h before oleate addition, and CCTα was localized by indirect immunofluorescence confocal microscopy (Figure 2A). Under basal conditions, CCTα was nucleoplasmic and contained within the nuclear lamina, which was visualized by immunofluorescence detection of lamin A/C. Addition of oleate resulted in CCTα translocation to the NE and discrete intranuclear structures that colocalized with lamin A/C. The frequency of these lamin-associated intranuclear foci increased with oleate treatment, with some cells containing three to four foci structures that seemed to be connected to the NE. In initial control experiments, we noted that the oleate carrier BSA (0.5%) had no effect on nuclear tubule formation. Figure 2B shows a magnified single section and projection of the entire nucleus of an oleate-treated CHO-K1 cell. The single section through the midregion of the nuclei revealed three to four large foci and several small structures that costained with lamin A/C and CCTα. A projection of the entire nucleus showed a complex network of large and small filaments containing both lamin A/C and CCTα.

To confirm that the observed CCTα- and lamin A/C-positive filaments represented an intranuclear membrane network, oleate-treated CHO-K1 cells were incubated with

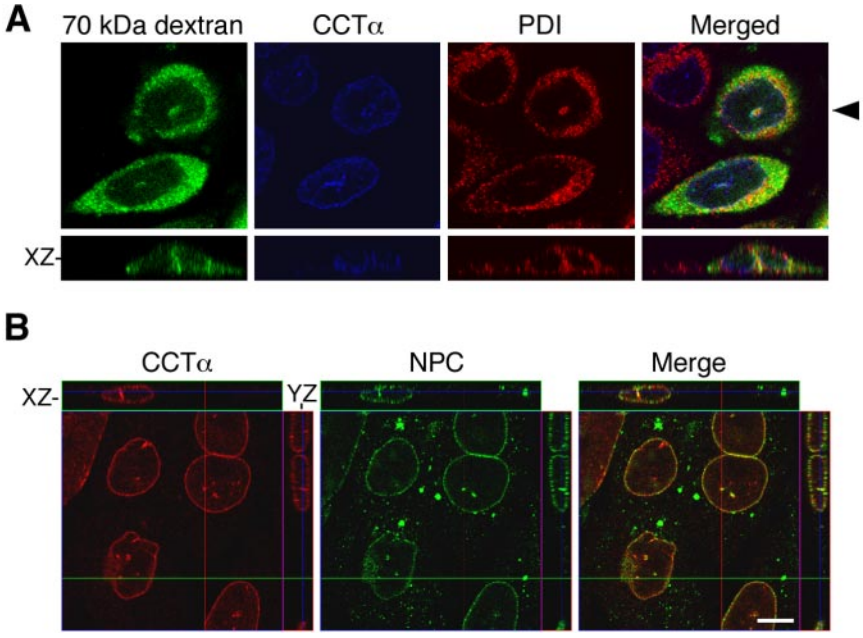

Figure 3. The nucleoplasmic reticulum of CHO-K1 cells contains cytoplasmic, ER and NE components. (A) CHO-K1 cells were treated for 4 h with oleate (500 μM), and the cytosolic compartment was visualized by scrape loading with Oregon green 488-conjugated dextran. CCTα and the luminal ER marker PDI were detected using secondary antibodies conjugated to Alexa647 and Alexa555, respectively. A single optical section in the XY plane is shown, whereas the XZ plane (position shown by arrowhead) was reconstructed from serial sections. (B) CCTα and nuclear pore complexes (Nup62 and related epitopes) were detected in CHO-K1 cells treated with oleate (500 μM) by using Alexa555- and Alexa488-conjugated secondary antibodies, respectively. A single optical section shows the XY plane, and XZ and YZ views were generated from reconstruction of serial sections. The green line shows the position of the XZ plane; the red line shows the position of the YZ plane. Bar, 10 μm.

fluorophore-conjugated Con A, which binds membrane glycoproteins on NE invaginations and is a sensitive marker for the NR (Fricker *et al*., 1997) (Figure 2C). Three-dimensional reconstruction of serial confocal sections through oleate-treated cells, viewed in the XZ and YZ planes, revealed filamentous nuclear structures labeled by fluorophore-conjugated Con A that colocalized with CCTα and lamin A/C. Nuclear invaginations of the NR were generally oriented vertically relative to the substrata and were frequently seen to completely traverse the nuclei.

The NR consists of invaginations of the double membrane of the NE and thus contains cytoplasm as well as luminal ER and NE constitutions. (Fricker *et al*., 1997; Echevarria *et al*., 2003). To assess whether CCTα-positive structures had cytoplasmic and ER markers, oleate-treated CHO-K1 cells were scrape loaded with Oregon green 488-conjugated dextran, a soluble cytoplasmic marker, and CCTα and the ER marker PDI were localized by immunofluorescence (Figure 3A). All three markers were colocalized within discrete intranuclear tubules in single optical sections through the midnuclear region. When confocal sections were reconstructed and viewed in the XZ-plane, all three markers occurred in tubules traversing the nucleus. The filamentous NR network visualized by immunostaining for CCTα colocalized with NPCs in single optical sections and in reconstructed images of the XZ-plane (Figure 3B). However, not all CCTα-positive structures contained NPCs. Collectively, these data show that CCTα translocates to a membranous network of tubules that has characteristics of the NR.

To investigate whether oleate-induced CCTα activation contributes to NR proliferation, NR tubules were quantified in control and oleate-treated CHO-K1 cells. The criteria for designating NR tubules in randomly selected fields of cells was based on either lamin A/C- or Con A-positive filamentous intranuclear structures continuous with the peripheral NE (described in *Materials and Methods*). Initially, lamin A/C-positive nuclear tubules that transversed 50% of the nucleus were quantified in images reconstructed from serial sections through the nucleus of control and oleate-treated CHO-K1 cells (Figure 4A). Using this method, oleate treatment caused an 80% increase in tubules. To facilitate tubule quantification in more cells, fluorophore-conjugated Con A was used to detect intranuclear foci in single confocal sections after it was confirmed that staining coincided with lamin A/C in three-dimensional reconstructions of nuclei (Figure 2C). Similar to results with lamin A/C, fluorophore-conjugated Con A-positive tubules increased by 60–70% after oleate treatment for 2 or 4 h (Figure 4B). The distribution of tubules/nuclei in the data set from Figure 4B for control and oleate-treated cells is shown in Figure 4C. A majority of untreated cells contained no or one tubule, whereas only 4% of cells had more than four tubules. After oleate treatment for 2 or 4 h, there was a 17–19% decrease in cells with no tubules and a corresponding increase in cells with two to four and more than four tubules (14 and 6%, respectively). In cells with more than four tubules per nuclei, there was no significant difference in mean number of tubules under any experimental condition (average number of tubules per nuclei: untreated, 5.5 ± 0.3; oleate 2 h, 5.5 ± 0.3; and oleate 4 h, 5.8 ± 0.2). This indicates that the increase in nuclear tubule frequency was not due to a subpopulation of cells with a disproportionately large number of tubules but rather to a shift in the overall distribution.

To determine whether NR proliferation in CHO-K1 cells was a general phenomena, the response to other fatty acids and in different acids cell lines was examined. Similar to oleate, treatment of CHO-K1 cells with arachidonate (200 μM) for 2 or 4 h significantly increased the number of Con A-positive nuclear tubules (Figure 4D). Nuclear tubule frequency also was increased significantly (~60%) by oleate in both F8 fibroblasts and NIH 3T3 cells (Figure 4E). CCTα translocated to intranuclear tubules in F8 and NIH 3T3 cells treated with oleate (our unpublished data).

CCTα Expression Caused NR Proliferation

To investigate the link between oleate-induced NR proliferation and CCTα activity, the effect of CCTα expression on nuclear tubule frequency was examined in CHO MT58 cells stably overexpressing rat CCTα (CHO58-CCT) and vector-transfected controls (CHO58-Vec) in the absence or presence of oleate. The parental CHO MT58 cells (Esko *et al*., 1981) and CHO58-Vec cells (Houweling *et al*., 1995) express a

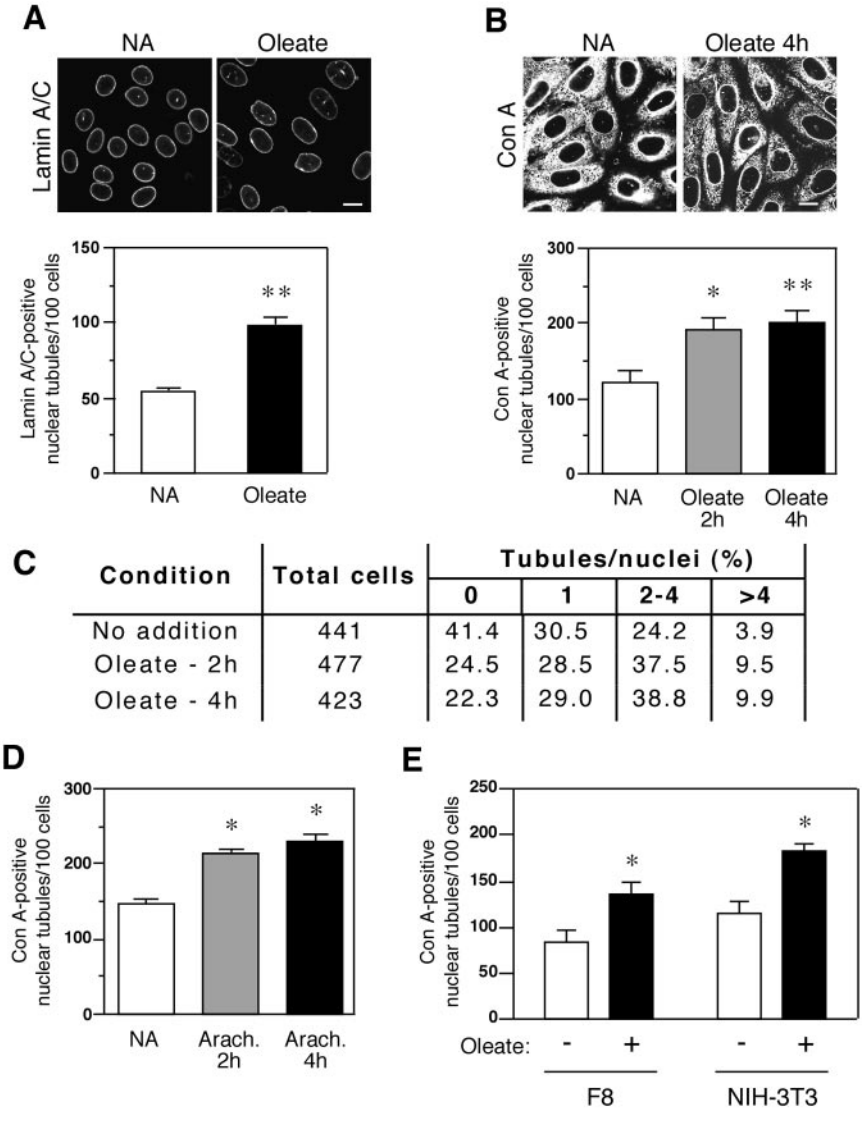

Figure 4. Proliferation of the nucleoplasmic reticulum in fatty acid-treated CHO-K1 cells. (A) Lamin A/C was detected in control and oleate-treated (500 μM for 4 h) CHO-K1 cells by using Alexa488-conjugated secondary antibody. Confocal microscopy and reconstruction of the nuclei from serial optical sections were used to collect data sets for the quantification of nuclear tubule frequency in cell populations as described in *Materials and Methods*. For these and all subsequent experiments, results are mean and SD from three separate determinations of >100 cells. $^{**}p < 0.01$. Bar, 10 μm. (B) Nuclear tubules in control and oleate-treated cells were visualized with Alexa488-conjugated Con A and quantified in single optical sections through the midnuclear region of cells, $^{*}p < 0.02$; $^{**}p < 0.005$. (C) Distribution of the numbers of tubules in individual nuclei from the data sets in B. (D) CHO-K1 cells were treated with 200 μM arachidonate for the indicated times, and nuclear tubule frequency was determined in fixed cells by using Alexa488-conjugated Con A; $^{*}p < 0.05$. (E) F8 and NIH 3T3 fibroblasts were treated with 500 μM oleate for 2 h. Con A-positive nuclear tubule frequency was determined as in B; $^{*}p < 0.05$.

temperature-sensitive CCTα allele that at 33°C provides sufficient activity and PtdCho synthesis to maintain cell viability. Immunoblot analysis showed that endogenous CCTα protein was virtually undetectable in CHO58-Vec cells at 37°C, thus providing a low background for comparison with CHO58-CCT cells (Figure 5A). In this and subsequent experiments (Figure 7), MT58 cells were not shifted to 40°C to ablate CCTα expression because 1) this is known to induce apoptosis (Cui *et al*., 1996), 2) the large temperature shift caused a heat shock response that altered nuclear morphology and affected CCT localization, and 3) experiments on endogenous CCT localization (Figures 2–4) also were done at 37°C. CCTα expression in CHO58-CCT cells was ~15-fold higher than in CHO-K1 cells. Consistent with elevated CCTα expression, CHO58-CCT cells also had a more than fourfold increase in [^{3}H]choline incorporation into PtdCho under basal conditions compared with CHO58-Vec cells (Figure 5B). PtdCho biosynthetic rates in both cell lines were stimulated approximately twofold by oleate treatment.

Next, the effect of CCTα expression on NR tubule frequency was quantified in CHO 58 cells. Endogenous CCTα in oleate-treated CHO58-Vec cells was undetectable by indirect immunofluorescence, and intranuclear Con A-staining was restricted to occasional NE invaginations (Figure 5C). In contrast, CCTα partially localized to the NE and strongly localized to the NR after oleate addition to CHO58-CCT cells. NR quantification by Con A staining revealed 65% more tubules in untreated CHO58-CCT cells relative to CHO58-Vec cells (Figure 5D). Oleate treatment increased nuclear tubule frequency by a further 150% in CHO58-CCT cells compared with only a 26% increase in CHO58-Vec cells. Analysis of the distribution of tubules per nuclei from data sets in Figure 5D indicated that the slight increase in nuclear tubules in CHO58-Vec cells after oleate treatment translated into an 11% decrease in cells with no nuclear tubules, and a corresponding increase in cells with one and two to four tubules (Figure 5E). In contrast, a 40% decrease oleate-treated CHO58-CCT cells with no and one nuclear tubule was accompanied by a proportional increase in cells with two to four and more than four tubules. Most notable was a sixfold increase in nuclei with more than four tubules in oleate versus untreated CHO58-CCT cells. This establishes that oleate-induced NR proliferation is enhanced by CCTα expression and/or the accompanying increase in PtdCho synthesis.

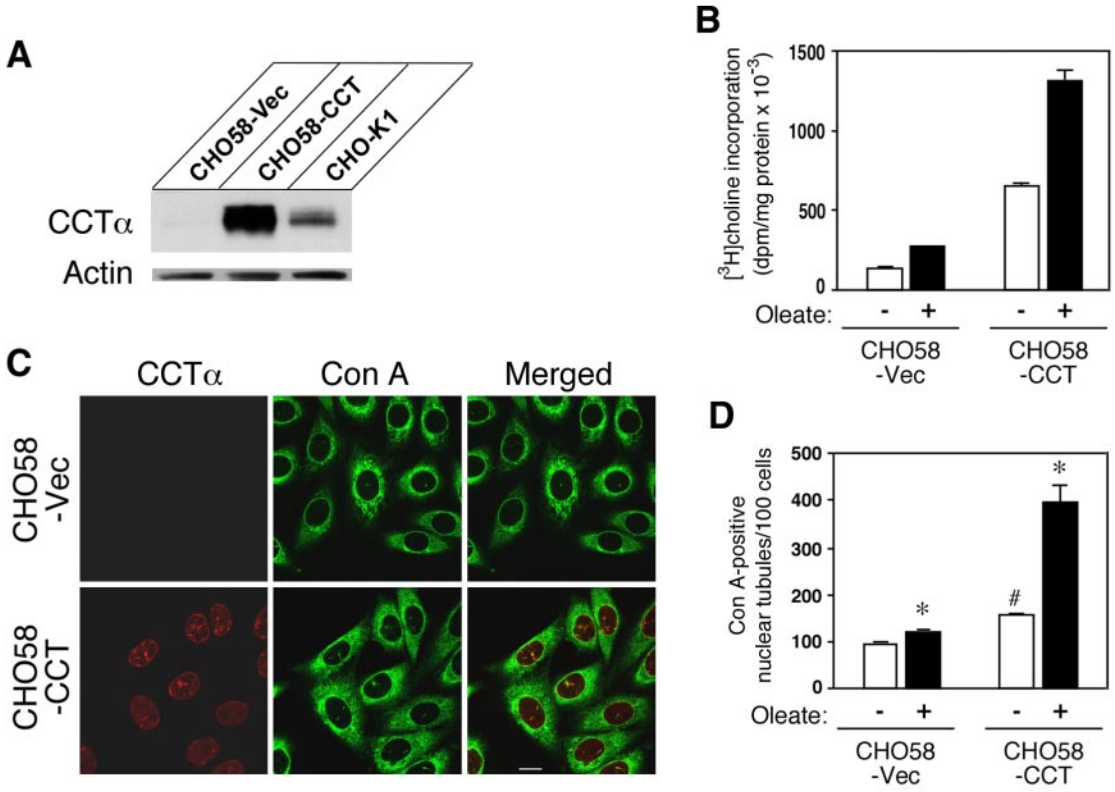

E

Cell Type	Condition	Total cells	Tubules/nuclei (%)			
			0	1	2-4	>4
CHO58-Vec	No addition	429	47.7	29.7	20.1	2.5
	Oleate - 2h	379	36.4	33.6	27.4	2.6
CHO58-CCTα	No addition	406	28.8	31.3	33.5	6.4
	Oleate - 2h	423	6.9	13.7	42.3	37.1

Figure 5. Proliferation of the nucleoplasmic reticulum is CCTα dependent. (A) CHO58-Vec and CHO58-CCT cells were cultured at 37°C for 2 h before harvesting total cell extracts for SDS-10% PAGE and immunoblot analysis of CCTα expression. Endogenous CCTα in CHO-K1 cell extracts is shown for comparison. Filters were stripped and probed for actin to demonstrate equal protein loading. (B) CHO58-Vec and CHO58-CCT cells were treated with 500 μM oleate or no addition for 2 h at 37°C. Cells received choline-free medium containing 2 μCi/ml [^{3}H]choline for the final hour, and isotope incorporation into PtdCho was measured. (C) Oleate-treated CHO58-Vec and CHO58-CCT cells were fixed, incubated with Alexa488-conjugated Con A, and immunostained for CCTα by using Alexa594-conjugated secondary antibody. (D) Frequency of total Con A-positive nuclear tubules in control and oleate-treated cells; #$p < 0.001$ compared with untreated vector-transfected controls; *$p < 0.05$ compared with no addition. (E) Distribution of numbers of tubules in individual cells from the data sets in D.

Ultrastructural analysis of the NR formed by CCTα activation and expression, as well as localization of CCTα, was determined by thin section EM and immunolabeling (Figure 6). There were two categories of double membrane intranuclear structures in control and oleate-treated CHO-K1 (Figure 6, A–D): 1) elongated cytoplasmic invaginations that were continuous with the inner and outer NE (Figure 6B), and 2) double membrane rings (~100–500 nm) within the nucleoplasm (Figure 6D). The spacing between the membrane rings was similar to that of the outer and inner NE, and occasional discontinuities along the double-layered membrane seemed to be NPCs (Figure 6D), indicating that these structures corresponded to horizontal cross-sectional views of cytoplasmic invaginations. This also is supported by a previous study that characterized these structures using serial-sectioning techniques (Fricker *et al*., 1997). NE invaginations were often in contact with nucleoli in control and oleate-treated cells (Figure 6A). Small circular single membranes characteristic of the ER were occasionally present within NE invaginations (Figure 6D).

Double membrane invaginations of the NE in CHO58-Vec and CHO58-CCT cells cultured in the absence or presence of oleate (Figure 6, E–L) were morphologically indistinguishable from those observed in CHO-K1 cells. Consistent with immunofluorescence data (Figure 5C), oleate-treated CHO58-CCT cells (Figure 6, K and L) contained abundant NE invaginations and tubules relative to untreated counterparts or CHO58-Vec cells. In addition, several unique features were associated with NE invaginations in oleate-treated CHO58-CCT cells. Arrays of unorganized tubular membrane clusters (TMCs) were observed in close association with the nucleoplasmic surface of double membrane

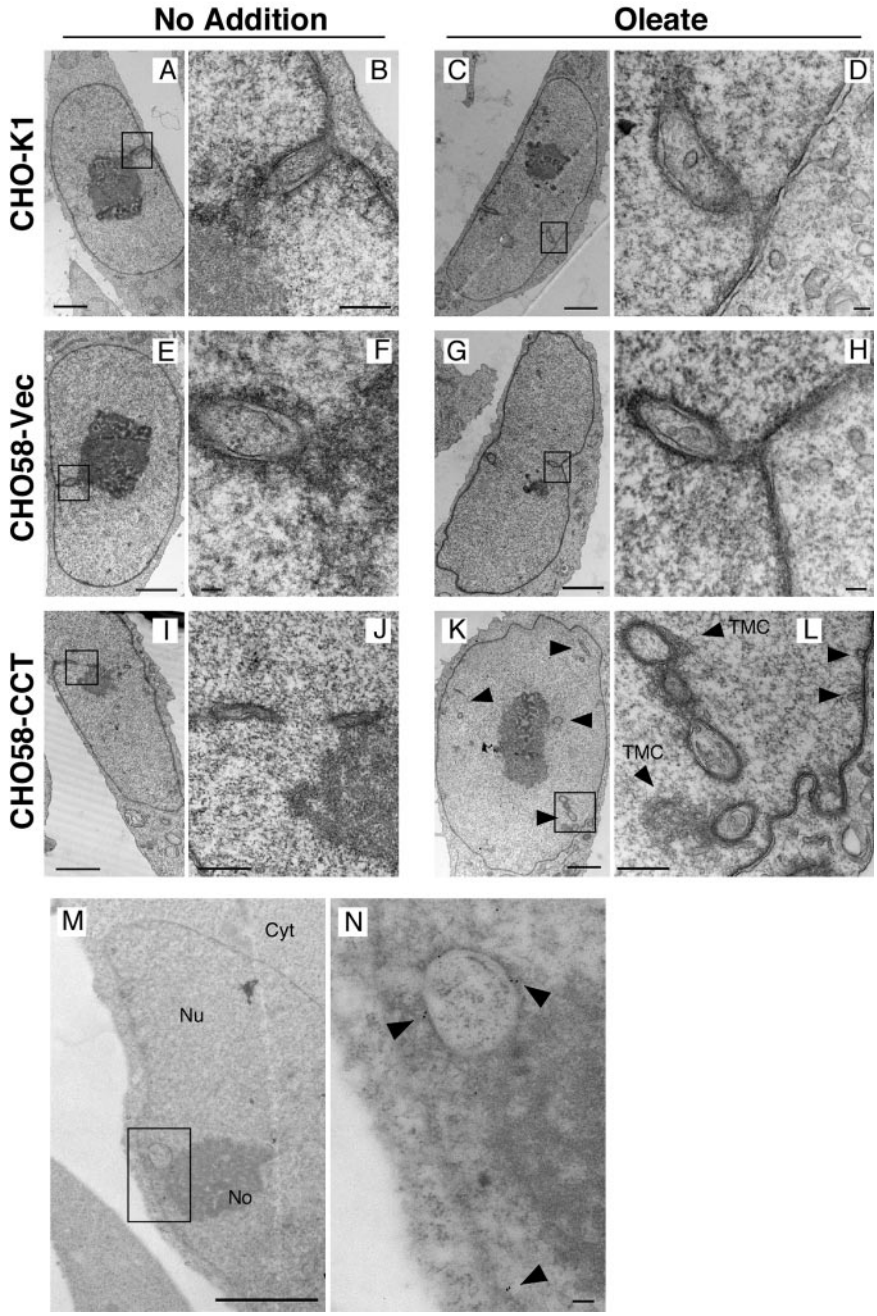

Figure 6. Effect of oleate and CCTα expression on ultrastructure of the nucleoplasmic reticulum. (A–D) CHO-K1 cells were incubated in the absence or presence of 500 μM oleate for 2 h and fixed, embedded, and sectioned for EM analysis. (E–L) CHO58-CCT or CHO58-Vec cells were treated with 500 μM oleate for 2 h and analyzed by EM. Low-magnification fields are shown in A, C, E, G, I, and K (bar, 2 μm) with selected high-magnification areas shown in B, D, F, H, J, and L (bar, 100 nm). Arrows in K indicate areas of abundant nuclear tubules and nuclear invaginations. (L) Arrows indicate TMCs and unique small invaginations of the NE. (M and N) CHO58-CCT cells were treated with oleate for 2 h, and CCTα was localized in embedded thin sections by immunogold labeling. Boxed area in M (bar, 2 μm) is shown at higher magnification in N (bar, 100 nm). Arrows in N indicate gold particles.

tubules (Figure 6L). Small invaginations of the inner nuclear membrane also were more frequently observed in CHO58-CCT cells treated with oleate (Figure 6L).

Although it is generally assumed that CCTα translocates to the nucleoplasmic surface of the NE after activation, whether CCTα is on the cytoplasmic or nucleoplasmic side of the NR unknown. Immunoelectron microscopy of CCTα in oleate-treated CHO58-CCT cells revealed that the enzyme was situated on the nucleoplasmic surface of the NR as indicted by gold particle clusters at this site (Figure 6, M and N). CCTα also was located on the nucleoplasmic surface of the NE.

CCTα Activity and Membrane Binding Increase Nuclear Tubule Formation

To determine the role of CCTα catalytic and membrane-binding activity in NR proliferation, domains responsible for these activities were mutagenized, and the NR network in CHO MT58 cells stably expressing the V5-tagged mutant proteins was analyzed (Figure 7). CCTα catalytic activity was ablated by mutation of the first residue of the active site HXGH motif involved in CTP binding (CCT H89G) (Veitch *et al*., 1998) or a lysine involved in catalysis (CCT K122A) (Helmink *et al*., 2003). Membrane-binding activity of CCTα was abolished by truncation at residue 236 (CCTΔ236), thus deleting the membrane-binding and phosphorylation domains and producing a soluble, constitutively active enzyme (Friesen *et al*., 1999) (Figure 1). CHO MT58 cells were stably transfected with the CCTα cDNAs or empty vector, and to eliminate possible clonal artifacts, pools of stably transfected cells (>100 clones/pool) cultured at 37°C were analyzed for CCTα expression and activity. SDS-PAGE and immunoblotting with a V5 and CCTα-specific

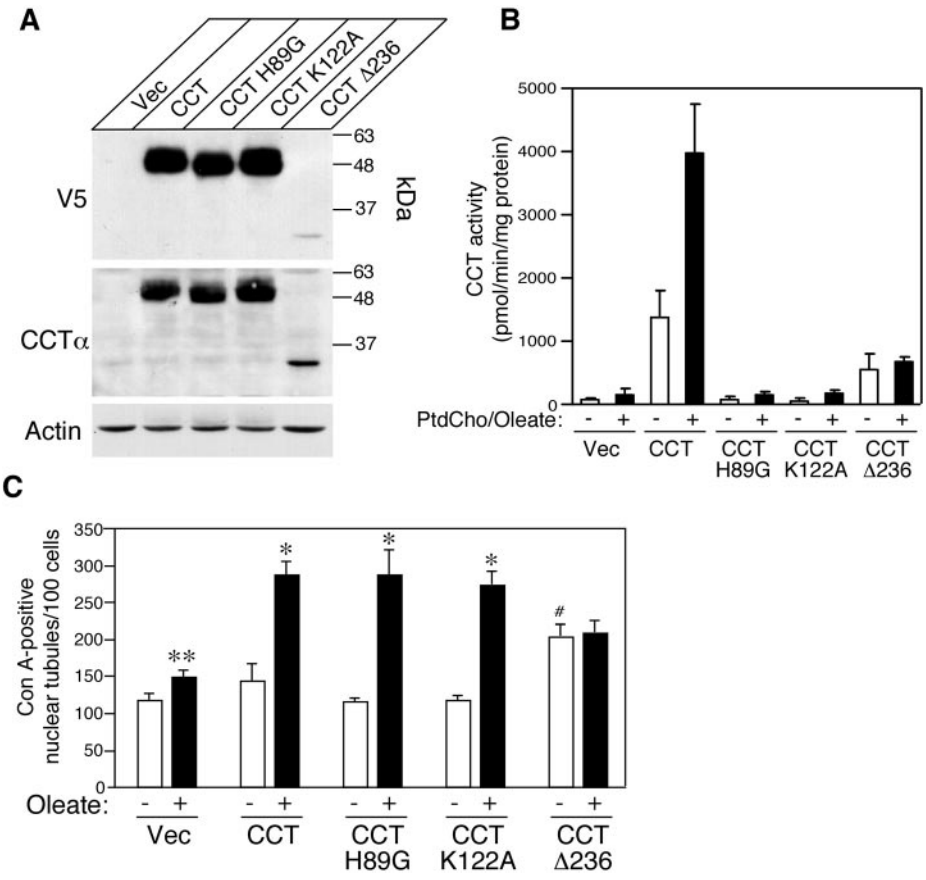

Figure 7. Induction of NR proliferation by catalytic-dead and membrane-binding–defective CCTα mutants. CHO M58 cells overexpressing wild-type or CCT H89G, K122A or Δ236 mutants were cultured at 37°C for 2 h before harvesting for experiments. (A) Expression of V5-tagged CCTα protein in stably transfected CHO MT58 cell was determined in whole cell extracts by SDS-10% PAGE and immunoblotting analysis with a V5-monoclonal antibody. The filter was stripped and reprobed with a CCT antibody directed against the N-terminus, followed by an actin antibody to demonstrate equal protein loading. (B) Total cell lysates from overexpressing CHO MT58 cells were assayed for CCT activity in the presence and absence of PtdCho/oleate vesicles. Data are the mean and SD for three experiments. (C) CHO MT58 cells stably expressing the indicated V5-tagged CCTα proteins were treated with or without 500 μM oleate for 2 h at 37°C. Frequency of Con A-positive nuclear tubules was determined in cells expressing V5-tagged CCTα; #$p < 0.05$ compared with untreated vector controls; *$p < 0.05$, **$p < 0.02$ compared with no addition.

antibody showed that wild-type CCT, CCT H89G, and CCT K122A were expressed at similar levels but significantly greater than CCTΔ236 (Figure 7A). Similar to results in Figure 5A, endogenous CCTα was expressed at low levels in vector control cells (Figure 7A). In vitro CCT assays of whole cell extracts showed that CCT H89G and K122A were catalytically dead, whereas wild-type activity was increased 17- and 26-fold in the absence or presence of PtdCho/vesicles, respectively (Figure 7B). In vitro activity of CCTΔ236 was increased approximately sevenfold compared with vector controls and was not further stimulated by addition of PtdCho/oleic acid vesicles. Measurement of PtdCho synthesis ([^{3}H]choline incorporation after treatment with or without oleate [500 μM] for 2 h) revealed that cells overexpressing wild-type CCTα displayed a 1.9- and 2.5-fold increase in PtdCho synthesis (relative to vector controls) in the absence and presence of oleate, respectively (mean of two experiments). PtdCho synthesis in cells expressing CCT H89G or K122A was similar to vector controls. However, relative to vector controls, overexpression of CCTΔ236 increased basal PtdCho synthesis by 2.4- and 2.5-fold in the absence and presence of oleate, respectively.

The extent of NR proliferation in cells expressing wild-type and mutant CCTα was determined by visualization of Con A-positive nuclear tubules in cells expressing V5-tagged CCTα (Figure S1) and the extent of NR proliferation was quantified (Figure 7C). Under basal conditions, expression of CCT H89G and CCT K122A had no effect on the frequency of nuclear tubules compared with wild-type and vector-transfected controls, whereas expression of CCTΔ236 increased NR tubules by 80%. Treatment with oleate for 2 h resulted in a slight increase in nuclear tubule frequency in vector-transfected control cells. In contrast, wild-type CCTα, CCT H89G, and CCT K122A translocated to the NR (Figure S1) and enhanced oleate-induced NE invaginations by ~100% (Figure 7C), indicating that CDP–choline formation and increased PtdCho synthesis was not a strict requirement for oleate-stimulated NE invagination. Oleate treatment of CCTΔ236-expressing cells did not further stimulate tubule formation, consistent with the lack of effect of oleate on membrane translocation and activity of this mutant (Figures 7B and S1).

Membrane Binding by CCTα Tubulates Liposomes

Enhanced proliferation of the NR in MT58 cells expressing catalytic-dead CCTα suggested that physical association of the enzyme with membranes could promote tubule formation. Several amphipathic proteins involved in membrane remodeling events in the cell, including dynamin, amphiphysin, and endophilin, cause evagination of liposomes into tubules through physical interaction with a lipid bilayer (Farsad and De Camilli, 2003). To test whether CCTα possessed similar activity, purified recombinant rat CCTα was incubated with liposomes prepared from total bovine brain lipids or a synthetic formulation, and liposome morphology was examined by negative staining and EM (Figure 8). To ensure that alterations in liposome morphology were not due to general effects of protein association, control incubations were carried out using the PH domain of oxysterol-binding protein fused to GST (GST-PH). Liposome sedimentation assays indicated that 30–50% CCTα and GST-PH bound to brain liposomes (Figure 8A). GST-PH bound quantitatively to synthetic liposomes enriched in PtdIns-4-P, compared with 30% binding of CCTα. The morphology of liposomes incubated with CCTα and the control protein were exam-

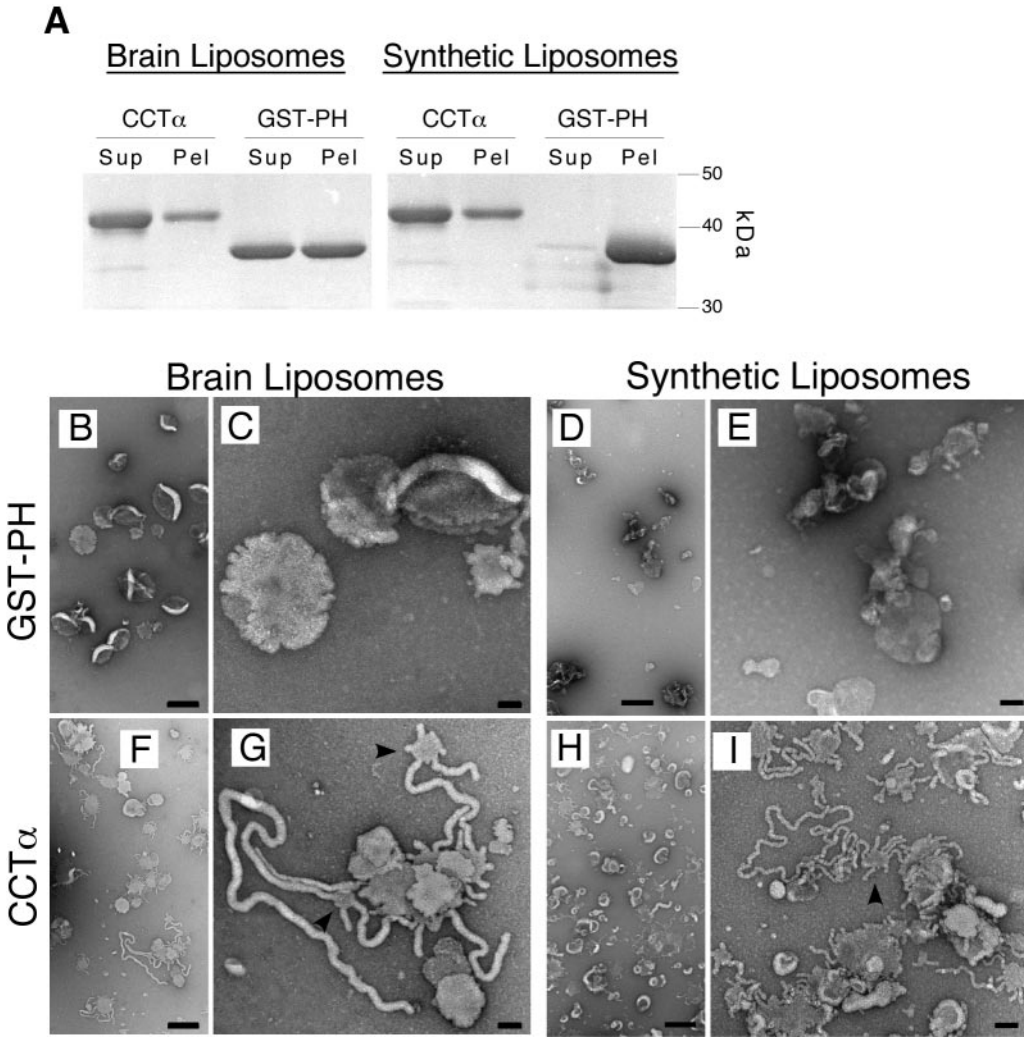

Figure 8. Tubulation of liposomes by purified recombinant CCTα. (A) Liposomes (250 μM) composed of total brain lipid extract or a synthetic formulation (50, 25, 17.5, 5, and 2.5 mol% of PtdCho, PtdEtn, PtdSer, oleic acid, and PtdIns-4-P, respectively) were incubated with purified recombinant CCTα or GST-PH (2.5 μM) and sedimented by high-speed centrifugation. Supernatant and pellet fractions were subjected to SDS-10% PAGE and proteins visualized by Coomassie staining. (B–I) Liposomes were incubated with recombinant proteins as described above and processed for EM. Low-magnification fields are shown in B, D, F, and H (bar, 500 nm) with adjacent selected high-magnification areas in C, E, G, and I (bar, 100 nm), respectively.

ined by negative staining and EM (Figure 8, B–I). The morphology of liposomes was not affected by incubation with GST-PH (Figure 8, B–E). However, EM analysis of liposomes incubated with CCTα revealed dramatic deformation of brain lipid and synthetic liposomes into thin tubules (Figure 8, F–I). The tubules formed by CCTα using brain liposomes had an average diameter of ~50 nm, compared with ~20 nm for the synthetic liposomes. The majority of tubules extended in a nonbranching array from a liposome; however, it was not uncommon to observe a tubule tethering large liposomes to small spherical bodies from which more tubules emanated (Figure 8, G and I, arrows). In the course of characterizing this activity, we noted that tubule formation was optimal when >1500 CCT molecules were bound per 400-nm vesicle. Moreover, vesicles composed of pure PtdCho and oleate [9:1 (mol/mol)] were less susceptible to tubulation, suggesting that negatively charged phospholipids and those that promote negative membrane curvature (phosphatidylethanolamine) contributed to tubule formation.

DISCUSSION

The NR extends deep into the nucleus and provides an interface for communication and transport between nuclear, cytoplasmic, and membrane compartments. Although it has been shown that the NR is a dynamic network that is variably expressed in different cell types (Fricker *et al*., 1997; Johnson *et al*., 2003b), the regulatory factors involved in its formation have not been identified. Here, we show that CCTα translocates to the NR and regulates its proliferation by mechanisms involving membrane binding and increased PtdCho synthesis.

Inactive CCTα has a nucleoplasmic distribution in many cultured cells (Wang *et al*., 1993, 1995; Lykidis *et al*., 1999). After oleate addition to CHO-K1, F8, and NIH 3T3 cells, CCTα was extensively translocated to the NE and tubular membrane structures. These tubules were identified as the NR based on 1) a double membrane continuous with the NE, 2) a cytoplasmic core, 3) associated lamina and NPCs, and 4) the presence of ER-resident proteins. The presence of cytoplasm, as well as ER

membrane and luminal markers, in the NR indicates that all three enzymes of the CDP–choline pathway and PtdCho synthesis necessary for membrane proliferation are consolidated at this site. In this model, activation of CCTα would promote translocation to the NR where the other two CDP–choline pathway enzymes reside, thus leading to localized production of PtdCho and expansion of NR membranes. The concept of CDP–choline pathway compartmentalization is supported by studies showing that the soluble intermediates phosphocholine and CDP-choline are nonexchangeable and channeled to the final product (George *et al*., 1989; Bladergroen *et al*., 1998). The exchange of soluble precursors between CK and CPT in the lumen and CCTα on nucleoplasmic surface of the NR could occur through NPCs. The fact that the NR is a cytoplasmic conduit composed of NE/ER membranes and has the capacity to make PtdCho provides a plausible explanation for a previous report of PtdCho synthesis in isolated nuclei (Hunt *et al*., 2001). It is possible that NR membranes and cytoplasm are inefficiently removed during nuclei fractionation, thus accounting for lipid metabolic activities associated with the nucleus.

Because CCTα translocated to both the NR and NE after oleate activation, it is feasible that PtdCho synthesis contributed to formation of new invaginations at the NE, as well as extension of preexisting tubules. In support of the former, CHO58-CCT cells treated with oleate showed evidence of small invaginations of the inner NE that could represent nucleation sites for tubule formation (Figure 6L). These short indentations in the NE cells could represent nascent tubules that did not fully extend due to limiting levels of another nuclear factor involved in NR formation. For example, under conditions of increased CCTα expression and membrane proliferation, lamins necessary for invagination of the NE might become limiting.

Consistent with a requirement for elevated PtdCho synthesis in NR proliferation, overexpression studies in CHO MT58 cells provided compelling evidence that increased NR tubule formation was dependent on CCTα expression and PtdCho synthesis (Figure 5). However, further analysis of CCTα mutants indicated that NR proliferation could be driven by both CCTα membrane binding and catalytic activity, as indicated by a 2- to 2.5-fold increase in NE invaginations in MT58 cells expressing catalytic-dead CCTα in the presence of oleate, and a twofold increase in invaginations in cells expressing constitutively active CCTΔ236 in the absence of oleate, respectively (Figure 7). Proliferation of the NR by CCT H89G and CCT K122A suggests that CCTα could directly alter membrane conformation to favor tubule formation. Because oleate was necessary for this effect, cellular levels of CCTα lipid activators would stimulate NR proliferation by a mechanism that was independent of PtdCho synthesis. Overexpression of CCT H89G or K122A did not stabilize or increase endogenous CCTα activity or PtdCho synthesis (Figure 7), indicating the observed effects on NR tubules were due solely to expression of the mutants. However, experiments shown in Figures 5 and 7 were performed at 37°C and not the nonpermissive temperature of 40°C that would have ablated PtdCho synthesis. Therefore, we cannot rule out the possibility that basal PtdCho synthesis contributed to NR formation by the catalytic-dead mutants.

In CHO MT58 cells, CCTΔ236 did not translocate to the NE, but it had constitutive activity as a result of removal of the inhibitory domain M (Wang and Kent, 1995). This CCTα mutant stimulated tubule formation in the absence of oleate, indicating that increased PtdCho synthesis alone promotes NR formation. Because the product of CCTα, CDP-choline, is soluble and presumably freely diffusible in the nucleus, increased PtdCho synthesis could take place wherever CPT activity is found. When overexpressed in CHO-K1 cells, choline/ethanolamine phosphotransferase was localized to the NE (Henneberry *et al*., 2002) and to NR tubules (Lagace and Ridgway, unpublished data), suggesting that PtdCho biosynthesis could occur at both membrane sites. Collectively, these data point to a mechanism for NR expansion that involves a coordinated effect of CCTα on membrane structure and activation of PtdCho synthesis.

Proliferation of the NR induced by oleate-dependent translocation of inactive CCTα H89G and K122A suggested that membrane binding via domain M contributed to tubule formation. The formation of extensive tubular evaginations of vesicles in vitro by purified CCTα in the absence of substrates showed that membrane-deforming properties of this enzyme could contribute to NR formation. Several other amphitrophic proteins have been shown to directly affect membrane curvature in vitro and in vivo. For example amphiphysin (Peter *et al*., 2004) and endophilin (Farsad *et al*., 2001) contain a membrane-deforming Bin/Amphiphysin/Rvs (BAR) domain (Peter *et al*., 2004). BAR domain-dependent membrane deformation occurs by electrostatic interactions with positive residues on the concave surface of the six-helix bundle dimer. CCTα does not contain a BAR domain, but specific lysine residues in the amphipathic α-helix are required for membrane binding in response to anionic lipids (Johnson *et al*., 2003a). Membrane tubulation by epsin has been proposed to occur by membrane insertion of the lipid-ordered amphipathic helical ENTH domain, thereby increasing the area of one monolayer and promoting evagination (Ford *et al*., 2002). Domain M of CCTα assumes an α-helical conformation upon lipid binding (Taneva *et al*., 2003) and could promote membrane tubulation in a similar manner. Immunolocalization of CCTα to the nucleoplasmic surface of the NR (Figure 6N) is topologically consistent with a role in tubulation of the inner bilayer of the NE double membrane. How increased positive curvature of the inner bilayer would deform the outer bilayer of the NR is unknown. Increased NR tubules in cells expressing membrane-binding defective CCT (Figure 7C) clearly shows that additional factors are required. These could include PtdCho production at the site of tubule formation, lipid composition, or the nuclear lamina, which is associated with the NR and is known to affect nuclear structure (Schirmer *et al*., 2001).

The NR is proposed to be involved in such essential functions as intranuclear Ca^{2+} signaling, gene expression, nuclear structural integrity, and nuclear-cytoplasmic transport. Our finding that CCTα promotes formation of the NR identifies a novel activity of CCTα and PtdCho synthesis that could ultimately affect these important nuclear functions.

ACKNOWLEDGMENTS

Robert Zwicker and Gladys Keddy provided technical assistance in tissue culture. Gary Faulkner and Mary-Ann Trevors assisted in EM analysis. This research was supported by a grant (MOP-62916) and salary award from the Canadian Institutes for Health Research (to N.D.R.). T.A.L. was supported by doctoral awards from K. M. Hunter/Canadian Institutes for Health Research and Cancer Research and Education in Nova Scotia.

REFERENCES

Attard, G. S., Templer, R. H., Smith, W. S., Hunt, A. N., and Jackowski, S. (2000). Modulation of CTP:phosphocholine cytidylyltransferase by membrane curvature elastic stress. Proc. Natl. Acad. Sci. USA *97*, 9032–9036.

Bigay, J., Gounon, P., Robineau, S., and Antonny, B. (2003). Lipid packing sensed by ArfGAP1 couples COPI coat disassembly to membrane bilayer curvature. Nature *426*, 563–566.

Bladergroen, B. A., Geelen, M. J. H., Reddy A. C. P., Declercq, P. E., and Van Golde, L. M. (1998). Channelling of intermediates in the biosynthesis of phosphatidylcholine and phosphatidylethanolamine in mammalian cells. Biochem. J. *334*, 511–517.

Broers, J. L., Machiels, B. M., van Eys, G. J., Kuijpers, H. J., Manders, E. M., van Driel, R., and Ramaekers, F. C. (1999). Dynamics of the nuclear lamina as monitored by GFP-tagged A-type lamins. J. Cell Sci. *112*, 3463–3475.

Cornell, R., and Vance, D. E. (1987). Translocation of CTP:phosphocholine cytidylyltransferase from cytosol to membranes in HeLa cells: stimulation by fatty acid, fatty alcohol, mono- and diacylglycerol. Biochim. Biophys. Acta *919*, 26–36.

Cornell, R. B. (1998). How cytidylyltransferase uses an amphipathic helix to sense membrane phospholipid composition. Biochem. Soc. Trans. *26*, 539–544.

Cornell, R. B., and Northwood, I. C. (2000). Regulation of CTP:phosphocholine cytidylyltransferase by amphitropism and relocalization. Trends Biochem. Sci. *25*, 441–447.

Cui, Z., Houweling, M., Chen, M. H., Record, M., Chap, H., Vance, D. E., and Terce, F. (1996). A genetic defect in phosphatidylcholine biosynthesis triggers apoptosis in CHO cells. J. Biol. Chem. *271*, 14668–14671.

de Figueiredo, P., Doody, A., Polizotto, R. S., Drecktrah, D., Wood, S., Banta, M., Strang, M. S., and Brown, W. J. (2001). Inhibition of transferrin recycling and endosome tubulation by phospholipase A2 antagonists. J. Biol. Chem. *276*, 47361–47370.

DeLong, C. J., Qin, L., and Cui, Z. (2000). Nuclear localization of enzymatically active green fluorescent protein-CTP:phosphocholine cytidylyltransferase alpha fusion protein is independent of cell cycle conditions and cell types. J. Biol. Chem. *275*, 32325–32330.

Drecktrah, D., Chambers, K., Racoosin, E. L., Cluett, E. B., Gucwa, A., Jackson, B., and Brown, W. J. (2003). Inhibition of a Golgi complex lysophospholipid acyltransferase induces membrane tubule formation and retrograde trafficking. Mol. Biol. Cell *14*, 3459–3469.

Echevarria, W., Leite, M. F., Guerra, M. T., Zipfel, W. R., and Nathanson, M. H. (2003). Regulation of calcium signals in the nucleus by a nucleoplasmic reticulum. Nat. Cell Biol. *5*, 440–446.

Esko, J. D., Wermuth, M. M., and Raetz, C. R. (1981). Thermolabile CDP-choline synthetase in an animal cell mutant defective in lecithin formation. J. Biol. Chem. *256*, 7388–7393.

Fang, M., Rivas, M. P., and Bankaitis, V. A. (1998). The contribution of lipids and lipid metabolism to cellular functions of the Golgi complex. Biochim. Biophys. Acta *1404*, 85–100.

Farsad, K., and De Camilli, P. (2003). Mechanisms of membrane deformation. Curr. Opin. Cell Biol. *15*, 372–381.

Farsad, K., Ringstad, N., Takei, K., Floyd, S. R., Rose, K., and De Camilli, P. (2001). Generation of high curvature membranes mediated by direct endophilin bilayer interactions. J. Cell Biol. *155*, 193–200.

Ford, M. G., Mills, I. G., Peter, B. J., Vallis, Y., Praefcke, G. J., Evans, P. R., and McMahon, H. T. (2002). Curvature of clathrin-coated pits driven by epsin. Nature *419*, 361–366.

Fricker, M., Hollinshead, M., White, N., and Vaux, D. (1997). Interphase nuclei of many mammalian cell types contain deep, dynamic, tubular membrane-bound invaginations of the nuclear envelope. J. Cell Biol. *136*, 531–544.

Friesen, J. A., Campbell, H. A., and Kent, C. (1999). Enzymatic and cellular characterization of a catalytic fragment of CTP:phosphocholine cytidylyltransferase alpha. J. Biol. Chem. *274*, 13384–13389.

Garduno, R. A., Faulkner, G., Trevors, M. A., Vats, N., and Hoffman, P. S. (1998). Immunolocalization of Hsp60 in Legionella pneumophila. J. Bacteriol. *180*, 505–513.

George, T. P., Morash, S. C., Cook, H. W., Byers, D. M., Palmer, F. B., and Spence, M. W. (1989). Phosphatidylcholine biosynthesis in cultured glioma cells: evidence for channeling of intermediates. Biochim. Biophys. Acta *1004*, 283–291.

Goldstein, J. L., Basu, S. K., and Brown, M. S. (1983). Receptor mediated endocytosis of low-density lipoprotein in cultured cells. Methods Enzymol. *98*, 241–260.

Helmink, B. A., Braker, J. D., Kent, C., and Friesen, J. A. (2003). Identification of lysine 122 and arginine 196 as important functional residues of rat CTP: phosphocholine cytidylyltransferase alpha. Biochemistry *42*, 5043–5051.

Henneberry, A. L., Wright, M. M., and McMaster, C. R. (2002). The major sites of cellular phospholipid synthesis and molecular determinants of Fatty Acid and lipid head group specificity. Mol. Biol. Cell *13*, 3148–3161.

Houweling, M., Cui, Z., and Vance, D. E. (1995). Expression of phosphatidylethanolamine N-methyltransferase-2 cannot compensate for an impaired CDP-choline pathway in mutant CHO cells. J. Biol. Chem. *270*, 16277–16282.

Hunt, A. N., Clark, G. T., Attard, G. S., and Postle, A. D. (2001). Highly saturated endonuclear phosphatidylcholine is synthesized in situ and colocated with CDP-choline pathway enzymes. J. Biol. Chem. *276*, 8492–8499.

Jackowski, S. (1996). Cell cycle regulation of membrane phospholipid metabolism. J. Biol. Chem. *271*, 20219–20222.

Johnson, J. E., Xie, M., Singh, L. M., Edge, R., and Cornell, R. B. (2003a). Both acidic and basic amino acids in an amphitropic enzyme, CTP:phosphocholine cytidylyltransferase, dictate its selectivity for anionic membranes. J. Biol. Chem. *278*, 514–522.

Johnson, N., Krebs, M., Boudreau, R., Giorgi, G., LeGros, M., and Larabell, C. (2003b). Actin-filled nuclear invaginations indicate degree of cell de-differentiation. Differentiation *71*, 414–424.

Kent, C. (1997). CTP:phosphocholine cytidylyltransferase. Biochim. Biophys. Acta *1348*, 79–90.

Lagace, T. A., Miller, J. R., and Ridgway, N. D. (2002). Caspase processing and nuclear export of CTP:phosphocholine cytidylyltransferase alpha during farnesol-Induced apoptosis. Mol. Cell. Biol. *22*, 4851–4862.

Lui, P. P., Lee, C. Y., Tsang, D., and Kong, S. K. (1998). Ca2+ is released from the nuclear tubular structure into nucleoplasm in C6 glioma cells after stimulation with phorbol ester. FEBS Lett. *432*, 82–87.

Lykidis, A., Baburina, I., and Jackowski, S. (1999). Distribution of CTP:phosphocholine cytidylyltransferase (CCT) isoforms. Identification of a new CCT-beta splice variant. J. Biol. Chem. *274*, 26992–27001.

Lykidis, A., and Jackowski, S. (2001). Regulation of mammalian cell membrane biosynthesis. Prog. Nucleic Acid Res. Mol. Biol. *65*, 361–393.

Northwood, I. C., Tong, A. H., Crawford, B., Drobnies, A. E., and Cornell, R. B. (1999). Shuttling of CTP:phosphocholine cytidylyltransferase between the nucleus and endoplasmic reticulum accompanies the wave of phosphatidylcholine synthesis during the G(0)→G(1) transition. J. Biol. Chem. *274*, 26240–26248.

Peter, B. J., Kent, H. M., Mills, I. G., Vallis, Y., Butler, P. J., Evans, P. R., and McMahon, H. T. (2004). BAR domains as sensors of membrane curvature: the amphiphysin BAR structure. Science *303*, 495–499.

Rothman, J. E., and Wieland, F. T. (1996). Protein sorting by transport vesicles. Science *272*, 227–234.

Schirmer, E. C., Guan, T., and Gerace, L. (2001). Involvement of the lamin rod domain in heterotypic lamin interactions important for nuclear organization. J. Cell Biol. *153*, 479–489.

Storey, M. K., Byers, D. M., Cook, H. W., and Ridgway, N. D. (1998). Cholesterol regulates oxysterol binding protein (OSBP) phosphorylation and Golgi localization in CHO cells: correlation with stimulation of sphingomyelin synthesis by 25-hydroxycholesterol. Biochem. J. *336*, 247–256.

Taneva, S., Johnson, J. E., and Cornell, R. B. (2003). Lipid-induced conformational switch in the membrane binding domain of CTP:phosphocholine cytidylyltransferase: a circular dichroism study. Biochemistry *42*, 11768–11776.

Veitch, D. P., Gilham, D., and Cornell, R. B. (1998). The role of histidine residues in the HXGH site of CTP:phosphocholine cytidylyltransferase in CTP binding and catalysis. Eur. J. Biochem. *255*, 227–234.

Wang, Y., and Kent, C. (1995). Identification of an inhibitory domain of CTP:phosphocholine cytidylyltransferase. J. Biol. Chem. *270*, 18948–18952.

Wang, Y., MacDonald, J. I., and Kent, C. (1993). Regulation of CTP:phosphocholine cytidylyltransferase in HeLa cells. Effect of oleate on phosphorylation and intracellular localization. J. Biol. Chem. *268*, 5512–5518.

Wang, Y., MacDonald, J. I., and Kent, C. (1995). Identification of the nuclear localization signal of rat liver CTP:phosphocholine cytidylyltransferase. J. Biol. Chem. *270*, 354–360.

Watkins, J. D., and Kent, C. (1992). Immunolocalization of membrane-associated CTP:phosphocholine cytidylyltransferase in phosphatidylcholine-deficient CHO cells. J. Biol. Chem. *267*, 5686–5692.

Wyles, J. P., McMaster, C. R., and Ridgway, N. D. (2002). Vesicle-associated membrane protein-associated protein-A (VAP-A) interacts with the oxysterol-binding protein to modify export from the endoplasmic reticulum. J. Biol. Chem. *277*, 29908–29918.

Yang, J., Wang, J., Tseu, I., Kuliszewski, M., Lee, W., and Post, M. (1997). Identification of an 11-residue portion of CTP-phosphocholine cytidylyltransferase that is required for enzyme-membrane interactions. Biochem. J. *325*, 29–38.